The structure of the phase transformation wave in the discrete model of a non-equilibrium phase transition

1995 J. Phys.: Condens. Matter 7 9173

(http://iopscience.iop.org/0953-8984/7/48/008)

J. Phys.: Condens. Matter 7 (1995) 9173–9184. Printed in the UK

The structure of the phase transformation wave in the discrete model of a non-equilibrium phase transition

S V Demishev†, T V Ischenko† and S J Blundell‡

† General Physics Institute, Submillimetre Spectroscopy Department, Vavilov Street 38, 117942 Moscow, Russia

‡ University of Oxford, Department of Physics, Clarendon Laboratory, Parks Road, Oxford OX1 3PU, UK

Received 21 June 1995, in final form 18 September 1995

Abstract. The structure of the wave of the phase transformation in the deterministic discrete model of non-equilibrium phase transitions is investigated. In this model each of the cells forming a two-dimensional lattice can be in one of three states: stable, metastable or excited. The transition into the stable state is allowed only through an intermediate excited state. The change of the phase state of each cell is initiated by the variation of a continuous parameter, the 'temperature', taking into account the energy exchange between cells, the phase stability regions and local rules in the neighbourhood of the cell. Taking the square and hexagonal lattices as examples, it is shown that this model possesses the following fundamental property: when the lifetime of the excited states is increased beyond a certain threshold, an abrupt change of the dynamics of the phase transition occurs. The wavefront then acquires a beam-like or fractal-like structure and, in the latter case, the system of cells has a quasicontinuous frequency spectrum of white or coloured noise. The application of this model to the description of non-equilibrium (explosive) crystallization in amorphous metals and semiconductors is discussed.

1. Introduction

There are two opposite approaches which are used for the theoretical description of non-equilibrium multiphase systems. The standard method [1, 2] consists in the solution of continuous differential equations which take into account the movements of the phase boundaries and the heat sources associated with them. This approach requires the self-consistent consideration of the temperature field and the corresponding distribution of the regions of different phase contents, and, as a result, the exact mathematical solution can be obtained only in the most simple limiting cases.

Another description of non-equilibrium systems is achieved through the discretization of the continuous dynamical variable and reduction of the global dynamics to the problem of the local interaction of discrete elements of the system with their nearest neighbours. This idea is the basis of the different cellular automata models which are now applied to the description of spin dynamics [3], seismic phenomena [4], hydrodynamical problems [5] and even to the non-linear transport of carriers in semiconductors [6]. However, the description of the dynamics of the phase transitions in the cellular automata approach is complicated and as far as we know has been performed only for spin-like systems in the neighbourhood of the percolation threshold [6–8].

The cellular automata approach may also give rise to the replacement of the continuous variable by a finite number of its discrete values and, consequently, to the problem of

0953-8984/95/489173+12$19.50

correspondence of the local rules to the exact microscopic physical model. A possible way to avoid this difficulty lies either in the increase of the number of grades of the discrete variable, or in the introduction of a continuous parameter whose variation will lead to discontinuous changes of the discrete system. In the latter case the model is no longer a classical cellular automaton [3, 11] but becomes intermediate between the two aforementioned approaches. It is this type of discrete–continuous model which has been applied to the description of the dynamics of earthquakes [4].

A similar approach was used in our work [9, 10] for the description of phase transitions in a mixture of stable and metastable phases. In this method [9, 10] the real medium is replaced by a discrete space consisting of cells having characteristic size L. The discrete variable is used to set the phase state of each element. The variation of the continuous variable, the temperature T, may induce changes of the phase state of each cell. From a formal point of view, each element (cell) of such a system is an elementary dynamical system with non-linear boundary conditions [10, 12], but in contrast to what is found in the standard non-linear systems [12] in our case the cells are arranged in an array and interact by the local rules characteristic of cellular automata models.

In our previous work we have shown that this model allows us to describe quantitatively the threshold characteristics for the excitation of non-equilibrium (explosive) crystallization in amorphous solids. At the same time we found that in certain cases the front of the phase transition may acquire a complicated fractal-like structure. The aim of the present work is to study the most general characteristics of the wave of the non-equilibrium phase transition in this model [9, 10], including an analysis of the different regimes of the wave propagation and instabilities on the wavefront.

2. Physical background and model formulation

Let us consider a wave of non-equilibrium (explosive) crystallization propagating in an amorphous film as a result of local pulsed energy deposition. The typical rate of this process is about $v = 10^2$–$10^3\ \mathrm{cm\,s^{-1}}$ [13], whereas the crystalline area from the viewpoint of the temperature profile can be considered as a thermal domain with the temperature much higher than that of the initial state and with the sharp front associated with the phase boundary.

Detailed analysis of the physical mechanisms of explosive crystallization [2, 10] indicates that it is insufficient to take into account only amorphous (metastable) and crystalline (stable) phases. It is necessary to consider also special excited states on the front of the phase transformation which, in accordance with [2, 10, 14], appear to be the high-energy vibrations of a disordered amorphous network localized at a length-scale $L \sim 1$ nm and having a lifetime $\tau \sim 10^{-9}$–10^{-10} s. Excitation of these states can be detected by specific effects on the optical properties [14] and results in (i) a drastic increase of the rate of crystallization and (ii) the equalizing of the rate of the dissipation of energy and the rate of the phase transition. The latter condition is necessary for a self-sustained wave of explosive crystallization. Hence in the approach of [2, 10, 14] the formation of these excited states becomes the necessary condition for the appearance of the fast phase transformations in amorphous materials.

This physical model can be formalized in the following way [2, 10, 14]. Each elemental volume of the sample is allowed to be in one of three phase states: stable (crystalline, 1 in figure 1(a)), metastable (amorphous, 2 in figure 1(a)) and excited (3 in figure 1(a)). We take the temperature T as the continuous dynamical variable whose variation induces the phase transitions and we will subsequently describe all energies in units of temperature

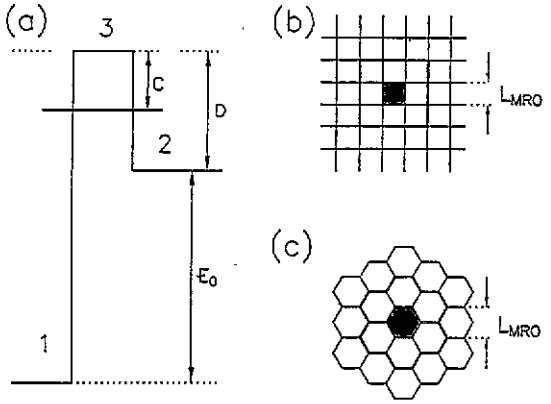

Figure 1. The energetic diagram in the discrete model of non-equilibrium phase transitions (a) and the structure of the nearest neighbourhood Ω_α (thick black line) for the square (b) and hexagonal (c) lattices (the central cell α is shaded).

[10]. The energy diagram, which determines the phase transitions (i.e. the change of the discrete variable), is shown in figure 1(a). The parameter D sets the region of stability of the metastable state (2): $T < D$. When $T = D$, the phase transition 2→3 to the excited state takes place with the jump of the temperature to the value $T = D + E_0$ (the heat of crystallization E_0 is released). In the process of the relaxation of the excited state (3) its temperature T decreases and at the point $T = D + E_0 - C$ the excited state becomes unstable and both the transitions 3→1 (to the stable crystalline state) and 3→2 (back to the metastable state) are possible. In the first case (3→1) T remains unchanged whereas in the second case (3→2) it is abruptly decreased by E_0. The transition 1→3 becomes possible at $T = E_0 + D$ and is not accompanied by any jump of T. It should be mentioned that direct transitions 2→1 and 1→2 are forbidden in the present model as a consequence of our assumption that the fast phase transition is controlled by the excited states [2, 10, 14].

Now we will assume that each elementary volume is one of the cells of the discrete space. The variation of the variable T_α for the cell with number α can be found by using the formula

$$\frac{dT_\alpha}{dt} = w \sum_{\beta \in \Omega_\alpha} (T_\beta - T_\alpha) \tag{1}$$

where summation is taken over the cells β which belong to the nearest neighbourhood, Ω_α, of the cell α. In the case of a phase transition, the T_α-value calculated in accordance with the formula (1) is modified in accordance with the rules described above. The parameter w corresponds to the characteristic frequency of the process $w \sim \tau^{-1}$.

It is worth discussing whether there are any physical foundations to the introduction of the discrete space or whether it is a purely formal procedure. In the case of amorphous semiconductors the characteristic spatial scale is given by the correlation length, or in other words by the medium-range-order length, $L_{MRO} \sim 1$ nm [15]. In some models of the amorphous state it is supposed that the amorphous solid can be described as an aggregate of more ordered 'rigid' regions of size $\sim L_{MRO}$ separated by more disordered 'soft' parts of random network [16]. In this approach the low-frequency anomalies of the Raman or neutron scattering spectra [17, 18] find their natural explanations. Besides, as we have shown previously [2, 14], in the case of excitation of the fast-crystallization wave the localization radius for the excited states becomes about L_{MRO}. Consequently in the framework of the

present approach it is reasonable to identify the size of the cell with the medium-range-order scale (figure 1).

In order to complete the formulation of the model, one needs to set up the local rule for the discrete variable in Ω_α. In our model the choice of the transition type at the decay of the excited state ($T = E_0 + D - C$) is controlled by the number of stable (crystalline) cells N_c in Ω_α: if $N_C \geqslant N_0$ then the transition 3→1 takes place and in the opposite case ($N_C < N_0$) we assume the 3→2 transition (figure 1). Hence the system of cells under consideration is fully deterministic and no stochastic rules are involved.

It is well established that in deterministic non-linear systems the smooth variation of the controlling parameter may induce the threshold appearance of complicated or chaotic dynamics [12]. For the present model, the preliminary results obtained in [10] have indicated that the variation of the parameter C, which sets the lifetime for the excited states (see figure 1(a): the larger C, the longer the relaxation time of the excited state), may lead to a complicated structure of the wavefront of the phase transformation. In the present work we will examine this case in more detail for square and hexagonal lattices (the corresponding Ω_α are shown in figure 1, (b) and (c); for the square lattice we have chosen the Moore neighbourhood). The numerical calculation procedure is described in detail in [10].

3. Results and discussion

Following [10] let us consider a flat interface between stable and metastable phases and introduce a point excitation on the boundary with temperature T_{ex}. The other cells have temperature $T = T_0$. If T_{ex} exceeds some critical value, a wave of crystallization begins to spread into the amorphous region [10]. The temperature field develops a sharp boundary, with temperature $T \sim E_0 + D$ within the crystallized or excited region, so the shape of the wave is not affected by the boundary conditions until it reaches the edge of the array [10].

We have taken the case where $E_0 = 100$, $D = 10$ and $T_0 = 9$; it was shown earlier [10] that the ratio $E_0/D \sim 10$ is characteristic for amorphous metallic films which undergo explosive crystallization [13]. The parameter N_0 in the local rule was set to $N_0 = 1$. The calculations were performed on a 100×100 array of cells.

To numerically calculate the time evolution of our model system, we have used the discrete analogue of equation (1). (The detailed procedure of this discretization has been described elsewhere [10].) In order to verify the accuracy of the calculation of the evolution of each pattern, the time-step was varied and decreased to the level where the quantitative characteristics of the non-equilibrium wave propagation become insensitive to the time-step. Below, we will consider results for both the wavefront structure and the character of the propagation which are independent of this time discretization.

3.1. The square lattice

The variation of the phase transition wave structure which takes place when the parameter C increases is shown in figure 2 (1–6). If C is less than some critical value, $C < C_1 = 0.6$, the wave has a distinct boundary and excited states always lie on it (figure 2, 2). Exceeding this critical value leads to a complicated fractal wavefront (figure 2, 3–5). This behaviour continues up to $C = C_2 = 1.7$ and for $C > C_2$ the motion becomes stable again with the difference that a wave of excitation states begin to spread into the amorphous region instead of a crystallization wave (figure 2, 6).

Qualitatively this change of regimes of the wave propagation can be explained by the change of ratio between the rate of dissipation and evolution of energy in the neighbourhood

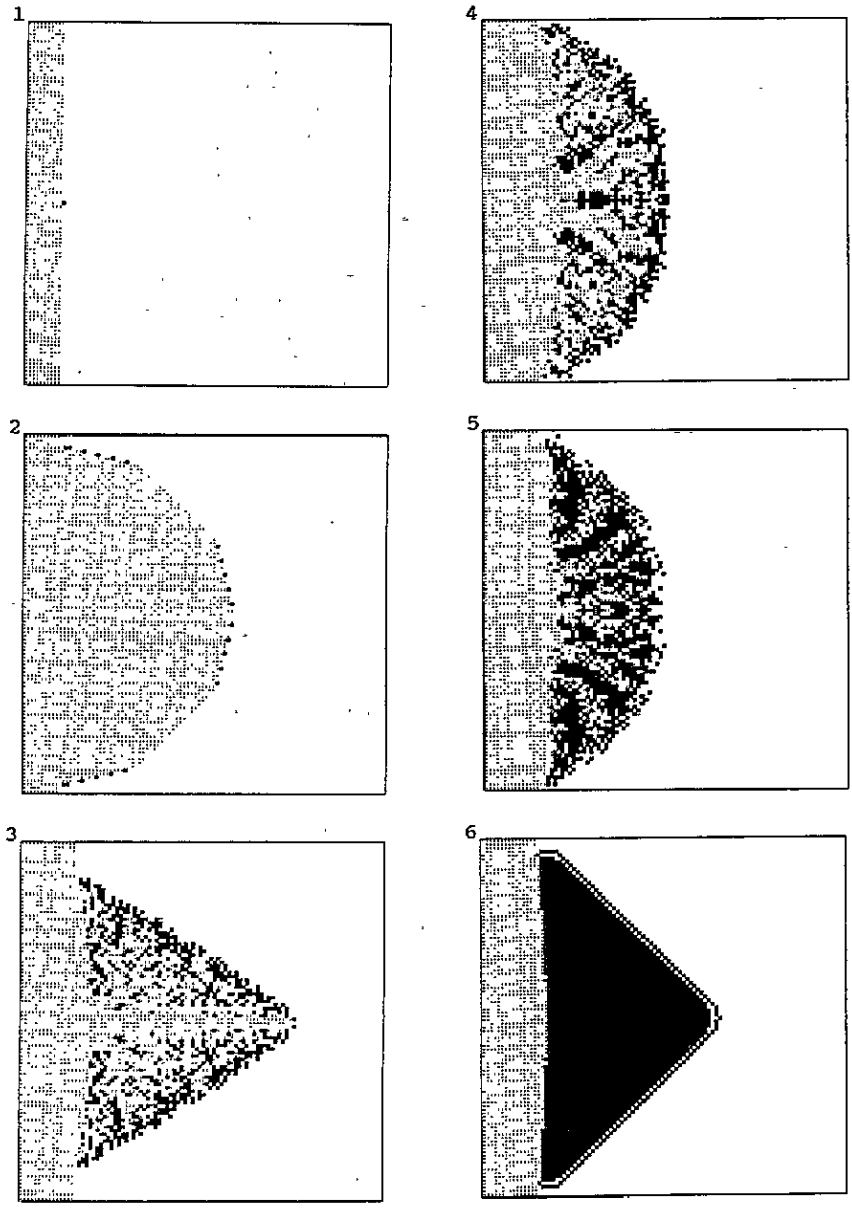

Figure 2. The structure of the wave of the non-equilibrium phase transformation on the square lattice. The metastable (amorphous) states are white, the excited states are black and the stable (crystalline) states are shaded. 1, initial state; 2, $C = 0.1$; 3, $C = 0.85$; 4, $C = 0.92$; 5, $C = 1.37$; 6, $C = 2$.

of the phase transformation. When the lifetime of the excited state is low (when parameter C is small) the cell with the high temperature is able to excite only its nearest neighbours and the wave has a stable front. On the boundary we have a flop-like process $2 \rightarrow 3 \rightarrow 1$ which controls the system dynamics (figure 2, 2). In the opposite limit of high C, when the lifetime of the excitation exceeds the dissipation time, $\tau \sim w^{-1}$, the cells are almost unable to cool down fast enough. According to the local rules the excited states will begin to

spread into the amorphous region and the characteristic transition will be of the 2→3 type. This process is accompanied by the slow movement of the stable phase boundary (figure 2, 6). In the intermediate case, when the rates of the energy dissipation and deposition are comparable the front instability appears when the excited and stable states become mixed (figure 2, 3–5).

Let us consider now the time evolution of the system. The total number of each kind of cell in the array $N_i(t)$ (where $i = 1, 2$ or 3) is given by the equation

$$N_i(t) = \bar{N}_i(t) + \delta N_i(t) \tag{2}$$

where $\bar{N}_i(t)$ is the average over a characteristic time period, $\bar{N}_i(t) = \langle N_i(t) \rangle$ representing the mean growth, and $\delta N_i(t)$ is an oscillating component for which $\langle \delta N_i(t) \rangle = 0$. The oscillating part is controlled by the dynamics of the transition process.

Within the accuracy of our calculations it is possible to approximate $\bar{N}_i(t)$ for various phases by using the power law

$$\bar{N}_i(t) \sim t^{\alpha} \tag{3}$$

where α is the growth dimensionality which is different for each particular case. This is clearly demonstrated by figure 3 where $\log N_1$ is plotted against $\log t$. The beginning of the $N_1(t)$-curve is controlled by the parameters of the initial excitation (figure 2, 1). After some time, the influence of the starting conditions becomes negligible and in this (quasistationary) limit the asymptotic behaviour follows equation (1). Similar plots were used to determine the growth dimensionalities for the excited and amorphous cells. The values of the indices α_1 and α_3 (for the crystalline and excited states respectively) are shown in figure 4 for different values of C.

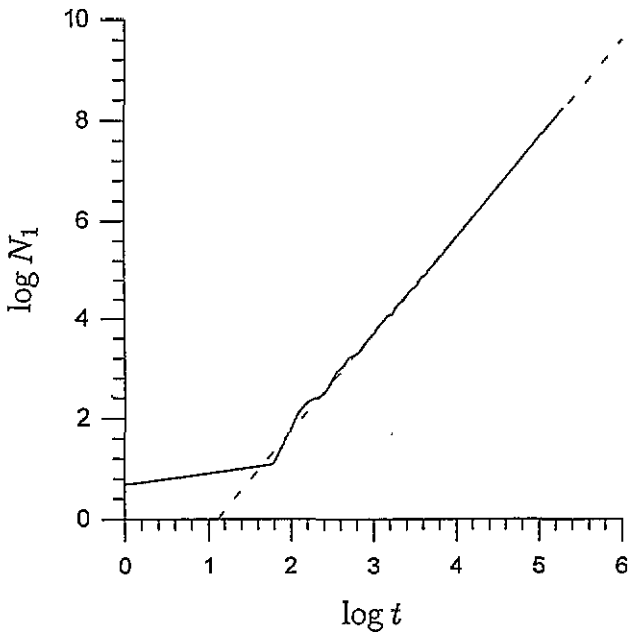

Figure 3. *The time dependence of the number of crystalline cells N_1 for the square lattice ($C = 0.2$).*

In the region where $C < C_1$ for the crystalline cells $\alpha_1 \sim 2$, whereas for the excited states $\alpha_3 \sim 1$. This behaviour corresponds to two-dimensional self-similar growth with

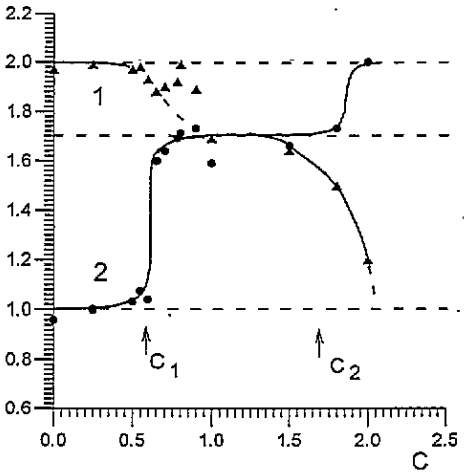

Figure 4. Growth dimensionalities on the square lattice for the different phases: 1, stable (crystalline) states (α_1); 2, excited states (α_3).

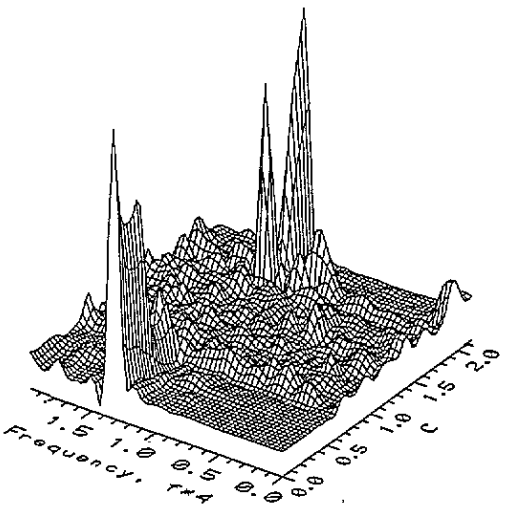

Figure 5. The evolution of the frequency spectra of the oscillating component for the square lattice.

constant velocity of stable states and to one-dimensional growth of the number of excited states located on the phase boundary respectively (figure 2, 2).

When the instability arises for $C > C_1$ the value of the α_3-index first jumps up to $\alpha_3 \sim 1.6$ and then in the region $0.6 \leqslant C \leqslant 0.9$ takes the asymptotic value $\alpha_3 \sim 1.7$ while the index $\alpha_1 \sim 1.8$–1.9. For the interval $0.9 \leqslant C \leqslant 1.7 \sim C_2$ both indices are close to ~ 1.7. For the values $C > C_2$ the situation becomes opposite to that for the range $C < C_1$, i.e. $\alpha_1 \sim 1$, whereas $\alpha_3 \sim 2$ (figure 4; figure 2, 6). It can be clearly seen from figures 2 and 3 that growth dimensions intermediate between 1 and 2 correlate with the excitation of fractal-like structure. It should be noted that the errors in the determination of the growth dimensionalities from the slope of the $\log N_1$ versus $\log t$ curves are different for the various regions of the parameter C. Away from the $C \sim C_1$ and $C \sim C_2$, where the motion is well established, the error is about 1% or less, whereas when $C \sim C_1$ or $C \sim C_2$, where the type of motion is changing, the error increases and can reach 10–15%. Similar error estimates are valid also for the hexagonal lattice (see below).

The variation of the spectral characteristics of the oscillating component $\delta N_3(t)$ for the excited states is shown in figure 5 (hereafter the frequency is given in units of w). In the range $C < C_1$ there is one dominating frequency in the spectrum, which can be attributed to the continuous process of excitation and relaxation on the wavefront.

Non-trivial behaviour is demonstrated in the region $C_1 < C < C_2$, where the spectrum acquires the character of white noise with the practically homogeneous filling of all of the frequency range (figure 5). This shows that on the square lattice, fractal-like structure is accompanied by a transition to chaotic dynamics in the oscillating component $\delta N_3(t)$. For $C > C_2$ the system dynamics becomes ordered again, with the dominating frequency close to the initial one observed for $C < C_1$. So the simple wave structure is unambiguously connected with the simple structure of the frequency spectrum (figure 5 and figure 2).

3.2. The hexagonal lattice

In the case of a hexagonal lattice we find that the variation of the transition wave structure with parameter C has a more complicated character than in the case of the square lattice. It is possible identify four different types of behaviour corresponding to four ranges of the parameter C (figures 6–8).

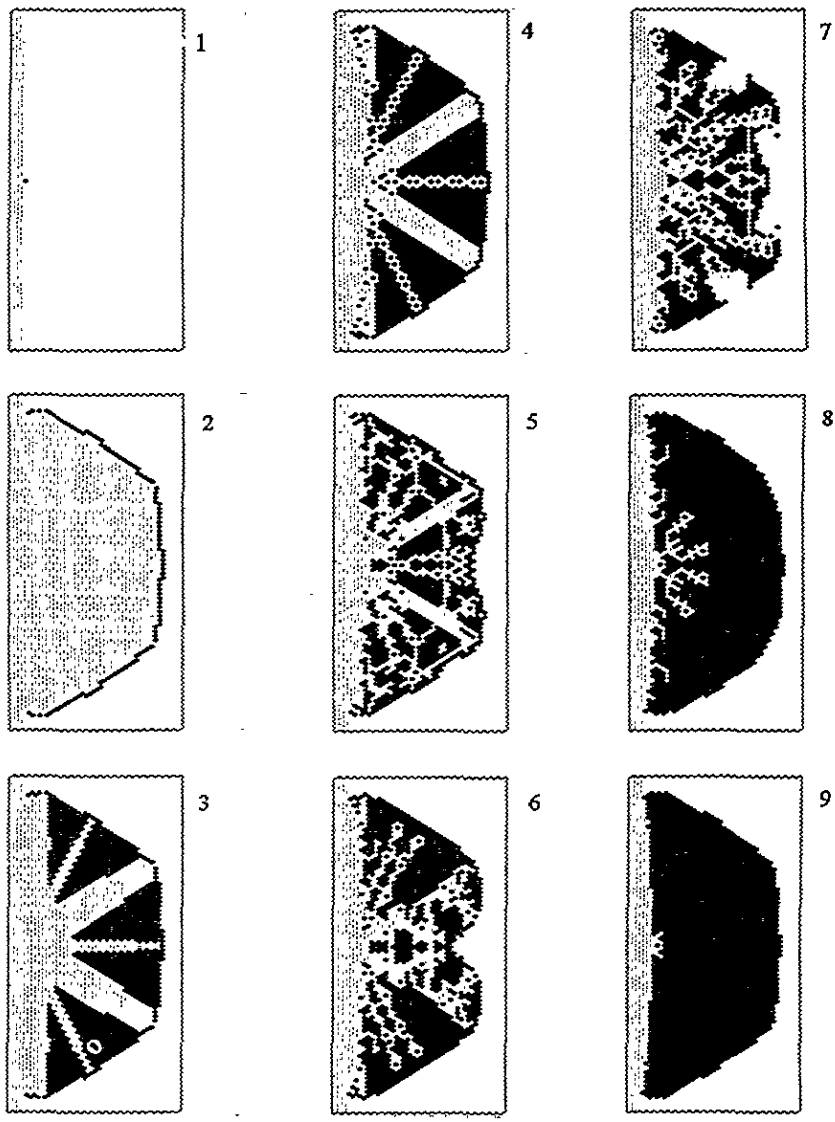

Figure 6. The structure of the wave of the non-equilibrium phase transformation on the hexagonal lattice. The cells are marked in the same way as on figure 2. 1, initial state; 2, $C = 0.98$; 3, $C = 1.01$; 4, $C = 1.10$; 5, $C = 1.11$; 6, $C = 1.15$; 7, $C = 1.18$; 8, $C = 1.27$; 9, $C = 1.36$.

In the interval $0 \leqslant C \leqslant 1.01$ (region I) the wave movement is stable, and fractal-like distortions are absent (figure 6, 2). Exceeding the critical value $C = 1.01$ leads to an abrupt variation of the structure of the phase transition wave: the growth of the crystalline phase

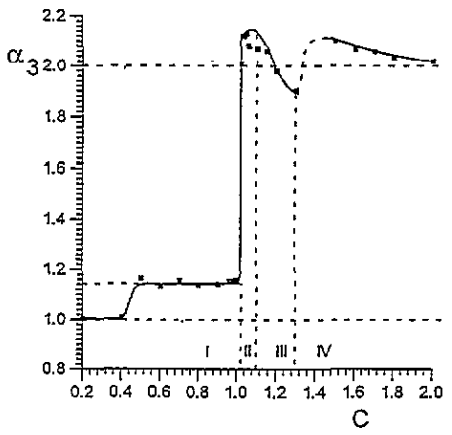

Figure 7. Growth dimensionality for the excited states on the hexagonal lattice.

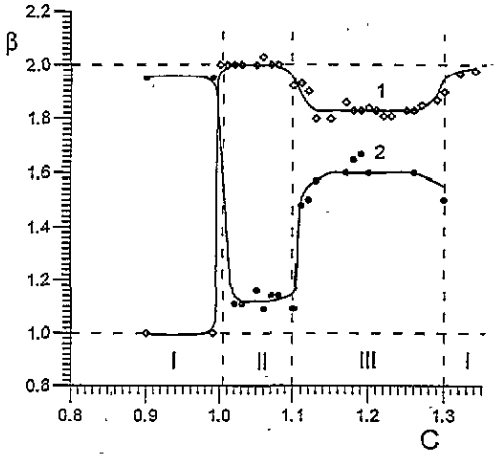

Figure 8. Space dimensionality for the different structures on the front of the wave of the phase transition for the hexagonal lattice. 1, excited states (β_3); 2, stable (crystalline) cells (β_1).

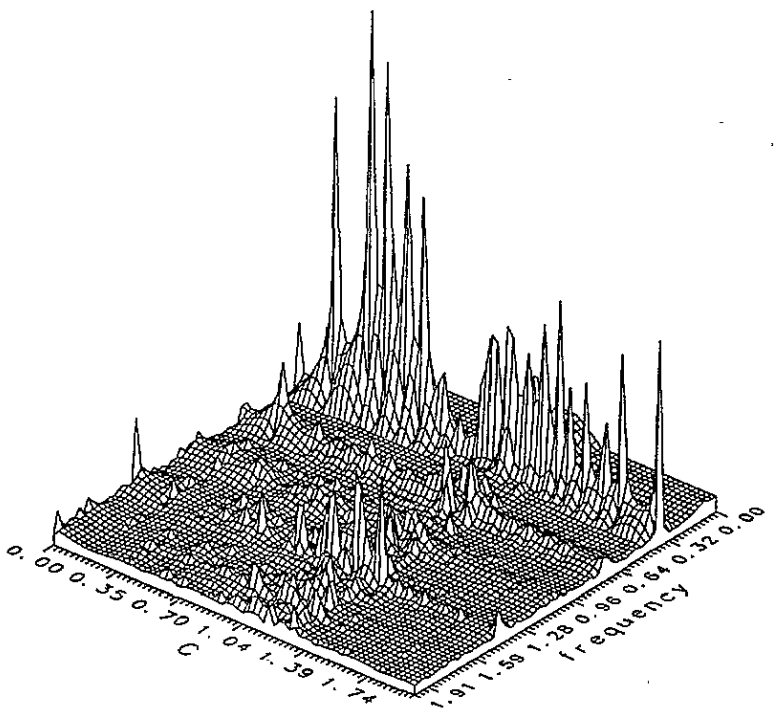

Figure 9. The evolution of the frequency spectra of the oscillating component for the hexagonal lattice.

appears to be aligned along several distinct directions outgoing from the initial point and as a result a beam-like structure is observed (figure 6, 3–4). This structure of the wave holds up to $C \sim 1.1$ (region II). In region III ($1.1 \leqslant C \leqslant 1.3$) the beam-like structure

become diffusive and the wave exhibits fractal structure (figure 6, 5–8). Further increase of the parameter C ($C > 1.3$, region IV) induces a change of the crystallization wave to the excitation type and the movement becomes stable (figure 6, 9).

The growth dimensionality α_3 for the excited states is shown in figure 7. It is interesting that for the hexagonal lattice even in region I a complicated behaviour is observed: for $C < 0.4$ the index α_3 takes the value $\alpha_3 = 1$, whereas for $C > 0.4$ the growth dimensionality increases up to $\alpha_3 \sim 1.14$.

The excitation of the beam-like structures leads to the jump of α_3 up to $\alpha_3 \sim 2.1$ in region II. In region III, where the wave is characterized by a fractal-like structure, the growth dimensionality decreases from $\alpha_3 \sim 2.1$ to $\alpha_3 \sim 1.9$ when the parameter C is varied in the interval $1.1 \leqslant C \leqslant 1.3$ (figure 7). The resumption of the stable motion (region IV) manifests itself in the growth of the α_3 to ~2.1. Further increase of the C-parameter in this area leads to the asymptotic value of the growth dimensionality $\alpha_3 = 2$ (figure 7).

Comparison of the data for the square and hexagonal lattices indicates that, firstly, the region of instabilities on the hexagonal lattice is narrower, and, secondly, there are values $\alpha_3 > 2$ characteristic of the hexagonal lattice. In order to explain the latter fact let us consider the spatial dimensionality β for the structures shown in figure 6, which are calculated according to the definition

$$N_i \sim r^{\beta} \tag{4}$$

where r is the distance from the point of initial excitation and N_i-values are taken at fixed time.

The results on the β-values (figure 8) show that the transition from region I to region II is accompanied by a stepwise decrease of the β_1-value for the crystalline (stable) states from $\beta_1 \sim 2$ to $\beta_1 \sim 1.1$. The latter value corresponds to the quasi-one-dimensional structure of the beams. At the same time in region II, for the excited states, we find that $\beta_3 = 2$. This space dimensionality can be obtained for the triangle structures (figure 6, 3) whose area is increased $\sim r^2$ due to geometrical similarity.

In region III the fractal-like structures can be characterized by the values $\beta_3 \sim 1.8$ and $\beta_1 \sim 1.55$ for the excited and crystalline states respectively. For $C > 1.3$ (region IV) the β_3-value is close to 2 as one should expect for the two-dimensional area (figure 6, 9).

Now we will introduce the velocity of the phase transition wave $v(t)$. Assuming $v(t) \sim t^{\gamma}$, after elementary integration one finds for the distance

$$r \sim t^{\gamma - 1}. \tag{5}$$

Combining the formulae (3)–(5) we find a connection between these indices:

$$\gamma = (\alpha - \beta)/\alpha. \tag{6}$$

It follows from the data in figure 7 and figure 8 that for $C < 0.4$ and $C > 1.8$ the index γ_3 for excited states is identically equal to zero, i.e. $v =$ constant (for the one-dimensional excited structures on the front of the phase transition in the region I we assume $\beta_3 = 1$). Also, within the interval $0.4 < C < 1.8$ the condition $\alpha_3 > \beta_3$ holds and consequently $\gamma_3 > 0$, i.e. the wave propagation accelerates. Estimates show that for the hexagonal lattice the γ-value lies in the range 0.05–0.15. However, the uncertainty in the values of α and β prevents us from determining whether the index γ depends on C. This question we leave for future investigations. It should be mentioned that this accelerated motion is characteristic only for the hexagonal lattice, whereas for the square lattice $v =$ constant and $\gamma = 0$.

The fundamental differences between the square and hexagonal lattices are also displayed in the structure of the frequency spectra for the oscillating component $\delta N_3(t)$ (figure 9). It is clearly seen that the characteristic discrete frequencies which determine

the process of cell excitation on the front of the phase transition can be observed over the whole range of the parameter C, including the interval of instabilities. It is interesting that at $C \sim 0.4$ the new component appears with frequency ~ 1.3 and this remains in the spectrum up to $C \sim 1.8$. This feature seems to correlate with the change of the type of the motion described above. We wish to emphasize that the maximum contribution from this frequency appears in the instability region (regions II and III).

From the data in figure 9 one can deduce that in the case of fractal-like motion (region IV) the noise is no longer white and the correlation with the frequencies which determine the system dynamics out of this region still holds in the spectrum. This is very different from the case of the square lattice (figure 5). We believe that this difference in behaviour may be connected with the different symmetry of the local neighbourhood Ω_α. Indeed, in our model for both hexagonal and square lattices, all the cells are equivalent with respect to the energy exchange (formula (1)), and also for the Moore neighbourhood (figure 1(b)) the corner cells and the cells which have a common edge are non-equivalent geometrically. Obviously for the hexagonal lattice all the cells are equivalent in both senses (figure 1(c)). Consequently we may suppose that the more developed chaotic dynamics and quasifractal structures in the case of the square lattice are possibly connected with the lower symmetry of the Moore neighbourhood.

4. Conclusion

We have shown that the discrete deterministic model for the non-equilibrium phase transitions based on consideration of the three states (stable, metastable and intermediate excited) and local rules as described above possesses the following fundamental property: beyond a certain threshold, an instability develops in the phase transition wave. This wavefront acquires a beam-like or fractal-like structure depending on the local lattice geometry and in the latter case the system exhibits the signs of chaotic dynamics—in particular, a quasicontinuous spectrum reminiscent of white or coloured noise. The character of this unstable and stochastic behaviour differs drastically between the square and hexagonal lattices and this may be connected with the difference in local symmetry, which affects the application of the local rules. The choice of the model parameters was made through comparison with values relating to explosive crystallization in amorphous metals. In this latter case, fluctuations accompanying the explosive crystallization wave propagation have been observed experimentally [19]. This may serve as an additional argument in favour of the description of non-equilibrium phase transitions which is developed in the present work. It is also possible that the beam-like structures observed for the hexagonal lattice correlate with experimental data for explosive crystallization of a-Si films [20] where beam-like structures were observed using electron microscopy. Another interesting matter concerns the order of the phase transition which occurs in both the square lattice and hexagonal lattice as the growth dimensionalities change and the motion changes regime. Unfortunately, the accuracy achieved in calculating properties in the transition regime is insufficient to deal with this question and we defer it to a future investigation.

Acknowledgments

The authors are grateful to F V Pirogov and to the referees for helpful comments, and to P D Karklin for his assistance in some calculations. This work was done in the framework of the 'Fullerenes and atomic clusters' program of the Ministry of Science of the Russian

Federation. SVD and SJB also acknowledge financial support from the Royal Society (UK) under a joint research project.

References

[1] Reynolds W N 1994 *Phys. Rev. Lett.* **72** 2797
[2] Demishev S V and Pirogov F V 1992 *Latvian J. Phys. Tech. Sci.* No 3 31
[3] Toffoli T and Margolus N 1987 *Cellular Automata Machines: a New Environment for Modelling* (Cambridge, MA: MIT Press)
[4] Olami Z, Feder H J S and Christinsen K 1992 *Phys. Rev. Lett.* **68** 1244
[5] Frish U, Haslacher B and Romeau Y 1986 *Phys. Rev. Lett.* **56** 1505
[6] Kometer K, Zandler G and Vogl P 1992 *Phys. Rev.* B **46** 1382
[7] Bray A J and Rutenburg A D 1994 *Phys. Rev.* E **49** R27
[8] Naeem J 1990 *J. Physique* **51** 201
[9] Demishev S V, Ischenko T V, Lyapin A G and Frolov S V 1990 *Izv. Acad. Nauk Latvian SSR* No 2 69 (in Russian)
[10] Demishev S V, Ischenko T V, Lyapin A G and Pirogov F V 1993 *J. Non-Cryst. Solids* **163** 13
[11] Packard N H and Wolfram S 1985 *J. Stat. Phys.* **38** 901
[12] Moon F C 1987 *Chaotic Vibrations* (New York: Wiley)
[13] Shklovskii V A and Kuz'menko V M 1989 *Usp. Fiz. Nauk* **157** 311 (in Russian)
[14] Demishev S V and Ischenko T V 1994 The modelling of the solid state amorphization *Preprint* The General Physics Institute, No 5
[15] Elliott S R 1991 *Nature* **354** 445
[16] Dembovskii S A and Chechetkina E A 1990 *Stekloobrasovaniye (Formation of Glasses)* (Moscow: Nauka) (in Russian)
[17] Pocsik I and Koos M 1988 *Disordered Systems and New Materials (Proc. 8th Int. School on Condensed Matter Physics)* (Varna: World Scientific) p 539
[18] Malinovsky V K, Novikov V N and Sokolov A P 1991 *Phys. Lett.* **153A** 63
[19] Kuz'menko V M and Mel'nikov V I 1982 *Zh. Eksp. Teor. Fiz.* **82** 802 (Engl. Transl. 1982 *Sov. Phys.–JETP* **55** 474)
[20] Bostanjoglo O and Schlotzhauer G 1981 *Phys. Status Solidi* a **68** 555